



Published in final edited form as:

*Mech Dev.* 2009 ; 126(5-6): 464–477. doi:10.1016/j.mod.2009.01.002.

## Small molecule screen for compounds that affect vascular development in the zebrafish retina

Satish S. Kitambi<sup>1,2,4</sup>, Kyle J. McCulloch, Randall T. Peterson<sup>3</sup>, and Jarema J. Malicki<sup>4,\*</sup>

<sup>1</sup> School of Life Sciences, Södertörns University College

<sup>2</sup> Department of Biosciences and Nutrition, Karolinska Institutet

<sup>3</sup> Cardiovascular Research Center, Massachusetts General Hospital

<sup>4</sup> Department of Ophthalmology, Harvard Medical School/MEEI 243 Charles Street, Boston, MA 02114, USA

### Abstract

Blood vessel formation in the vertebrate eye is a precisely regulated process. In the human retina, both an excess and a deficiency of blood vessels may lead to a loss of vision. To gain insight into the molecular basis of vessel formation in the vertebrate retina and to develop pharmacological means of manipulating this process in a living organism, we further characterized the embryonic zebrafish eye vasculature, and performed a small molecule screen for compounds that affect blood vessel morphogenesis. The screening of approximately 2000 compounds revealed four small molecules that at specific concentrations affect retinal vessel morphology but do not produce obvious changes in trunk vessels, or in the neuronal architecture of the retina. Of these, two induce a pronounced widening of vessel diameter without a substantial loss of vessel number, one compound produces a loss of retinal blood vessels accompanied by a mild increase of their diameter, and finally one other generates a severe loss of retinal vessels. This work demonstrates the utility of zebrafish as a screening tool for small molecules that affect eye vasculature and presents several compounds of potential therapeutic importance.

### Keywords

Blood; Circulation; Intraocular; Hyaloid; Vasculature; Angiogenesis; Chemical; Disease

### 1. Introduction

The zebrafish has gained considerable importance as a model for the studies of vertebrate development. The small size, rapid external embryogenesis, and the transparency of the embryo during early stages of embryogenesis all benefit the efforts to use this organism in developmental studies (Kimmel et al., 1995). Similarly, the identification of hundreds of mutant strains facilitates the study of genetic process that regulate development (Amsterdam et al., 2004; Driever et al., 1996; Haffter et al., 1996). More recently, the sequencing of the genome and the availability of reverse genetic methods further strengthened the zebrafish

\*corresponding author: Tel: +1 617 573 4372, Fax: +1 617 573 4290, email: jarema\_malicki@meei.harvard.edu.

**Publisher's Disclaimer:** This is a PDF file of an unedited manuscript that has been accepted for publication. As a service to our customers we are providing this early version of the manuscript. The manuscript will undergo copyediting, typesetting, and review of the resulting proof before it is published in its final citable form. Please note that during the production process errors may be discovered which could affect the content, and all legal disclaimers that apply to the journal pertain.

model (Nasevicius and Ekker, 2000; Wienholds et al., 2002). Importantly, the same characteristics that make the zebrafish suitable for genetic experiments: small size, rapid development, and transparency, make it also exceptionally useful for small molecule screens (Peterson et al., 2000; Tran et al., 2007; Zon and Peterson, 2005). In these studies, small batches of embryos are exposed to many thousands of different chemical compounds and analyzed for developmental changes. Such an approach can be applied either to wild-type embryos or to carriers of genetic defects that phenocopy human abnormalities. In the latter case, it can be a powerful way to identify chemicals of potential therapeutic importance (North et al., 2007).

In the eyes of most vertebrates, an intricate network of blood vessels supplies oxygen and nutrients to the retina. The importance of this system is underscored by the fact that retinal vascularization defects are seen in many human diseases (Grunwald et al., 1998; Killingsworth et al., 1990; Ross et al., 1998; Weber et al., 1994). The hyaloid, retinal, and choroidal vasculatures are the three main blood supply systems in the eye of most mammals. The hyaloid vasculature is the first to form and exists transiently only (Saint-Geniez and D'Amore, 2004). Hyaloid vessels enter the retina through the optic fissure and form a dense network around the lens. Later during development, hyaloid vessels regress and are replaced by the retinal vasculature (Saint-Geniez and D'Amore, 2004; Smith, 2004; Zhu et al., 1999). The genes *Wnt7b*, *Fz4*, and *Lrp5*, have been shown to regulate this process in mice (Kato et al., 2002; Lang and Bishop, 1993; Lobov et al., 2005; Xu et al., 2004). Failure of hyaloid regression in the human eye (Smith, 2004; Zhu et al., 1999) leads to a pathological condition known as persistent fetal vasculature (PFV) (Goldberg, 1997). The vasculature of the mature mammalian eye consists of two separate blood vessel networks: the retinal and the choroidal vasculature. The first of these is made up of two components: the superficial primary, and the deep secondary vessel system (Kato et al., 2002; Lang and Bishop, 1993; Xu et al., 2004). The deeper plexus originates from the primary one as vessels that penetrate into the layers of retinal neurons and branch along the inner and outer surfaces of the inner nuclear layer (Kato et al., 2002; Lang and Bishop, 1993; Xu et al., 2004). Finally, the choroidal circulation is closely associated with the pigmented epithelium and in most mammals supplies oxygen and nutrients to the photoreceptor cell layer. Defects in this set of vessels are associated with Age-Related Macular Degeneration (AMD) (Grunwald et al., 1998).

Efforts to characterize the zebrafish retinal vasculature revealed that a network of vessels first forms between the retina and the lens, similar to many other vertebrates (Alvarez et al., 2007). In contrast to retinae of many mammals, however, it is thought that the embryonic vasculature of the zebrafish eye does not degenerate and instead transitions into a mature vascular network. Moreover, the retinal vasculature appears to be confined to the inner surface of the retina, as deep vessels embedded into layers of retinal neurons have not been reported. Several chemically-induced zebrafish mutants display retinal vessel defects, providing an opportunity to study the genetic basis of vasculature formation (Alvarez et al., 2007). Here we use two zebrafish transgenic lines; *fli1:EGFP*, and *flkl:GFP* (Choi et al., 2007; Lawson and Weinstein, 2002), to further investigate the development of retinal vasculature, and to demonstrate that zebrafish embryos can be effectively used in small molecule screens to identify medically-relevant compounds affecting blood vessel development in the eye.

## 2. Results

### 2.1. Vasculature development in the wild-type retina

The zebrafish optic primordium evaginates from the forebrain region around the 6–7 somite stage, takes up a wing-like shape by the 9-somite stage, and reorients its position to achieve a vertical orientation by 12 somites (reviewed in Avanesov and Malicki, 2004). Following that, the eye cup invaginates and the choroid fissure forms at the anterior rim of the eye by the 20 somite stage, or ca. 18 hours postfertilization (hpf). Throughout early embryogenesis, the eye

primordium consists of mitotically active cells. The first to become postmitotic are ganglion cell progenitors, which exit the cell cycle at around 27 hpf, marking the onset of retinal neurogenesis (Hu and Easter, 1999; Nawrocki, 1985). This is followed by the appearance of interneurons and photoreceptor cells, resulting in a functional retina by ca. 3 dpf (Easter and Nicola, 1996). It is not well understood how these events correlate with the appearance of the retinal vasculature. Previous studies reported that blood vessels are present around the medial side of the lens by 60 hpf, and gradually spread laterally to cover most of the lens surface (Alvarez et al., 2007). To our knowledge, earlier events have not been, however, described so far.

To determine the onset of blood vessel formation during early eye morphogenesis, we used two transgenic lines that express fluorescent reporter proteins in the vascular system: the *fli1:EGFP* line that carries the EGFP gene driven by the *fli1* promoter (Lawson and Weinstein, 2002), and the *flkl1:GFP* line, expressing GFP under the control of the *flkl1* regulatory sequences (Choi et al., 2007). The *fli1* gene encodes an ETS family transcription factor expressed in the ventral mesoderm by 12 hpf, and subsequently detected in all the endothelial vessels (Melet et al., 1996; Meyer et al., 1993; Thompson et al., 1998). The zebrafish *flkl1* is a homologue of the mammalian VEGF receptor, KDR, belongs to the family of receptor tyrosine kinases, and is also expressed at early stages of blood vessel formation (Choi et al., 2007; Thompson et al., 1998). The two transgenic lines display similar, if not identical, GFP expression patterns in the retina. We first investigated *fli1:EGFP* expression at 18 hpf and found that as previously reported it is present in cranial and trunk blood vessels. We did not, however, detect GFP signal in the zebrafish eye at this stage (Fig. 1A), indicating that the vasculature is most likely absent. By 24 hpf, however, *fli1:EGFP*-positive cells are seen in the choroid fissure area and behind the lens (Fig. 1B). This expression pattern suggests that the *fli1:EGFP* cells may enter the retina through choroid fissure. By 28 hpf, the GFP-positive cells appear to extend inward from the choroid fissure and occupy an area behind the lens (Fig. 1C). These cells most likely form the first rudiment of the retinal vasculature, hereafter referred to as the intraocular vasculature. At about the same time, a group of GFP-positive cells appears on the retinal surface directly opposite to the choroid fissure region, in the so-called posterior groove region (red arrow in Fig. 1C). These cells are likely to contribute to the surface vasculature that is described below.

By 48 hpf, a network of vessels surrounds the medial side of the zebrafish lens (Fig. 1D, E). During the next 24 hours, this network expands towards lens equator, where it merges into a single intraocular ring vessel that runs around the lens (red arrowheads in Fig. 1D, E, G, H, J, K and Fig. 2D, F). During the same period, a vessel system forms on the external surface of the developing zebrafish eye. It includes three radial vessels, here designated as the nasal, the dorsal, and the ventral radial vessel (red arrows in Fig. 1F), which merge into another ring vessel around the lens circumference, in this case on the surface of the eye. The intraocular and surface vessel systems connect through a single duct that extends from the ventral region of the intraocular vasculature and connects to the surface ring vessel in the vicinity of its junction with the ventral radial vessel (asterisk in Fig. 1D, G, H, I and in Fig. 2B, C).

Between 48 and 144 hpf, intraocular vessels undergo remodeling so that their trajectories become less convoluted (Fig. 1D–K and Fig. 2D, F). At 144 hpf, the arrangement of vessels around the lens resembles fingers holding a tennis ball (Fig. 1K). A similar radial configuration of intraocular vessels is seen at 30 dpf (Fig. 1N), and becomes even more obvious in adult individuals (Alvarez et al., 2007). Although we did not follow this segment of vasculature in detail, we note that choroidal vessels form a dense polygonal network enveloping the outer surface of the eye by 9 dpf (Fig. 1M and Fig. 2E).

Blood circulation in the retina is clearly visible by 72 hpf both in the surface (yellow arrows in Fig. 1F, movie 1) and in the intraocular vessels (movie 2). In the intraocular vasculature

system, blood is supplied by a single duct that runs along the optic nerve (white arrows in Fig. 1I, K), flows around the lens and then is directed through the connecting vessel into the surface vasculature (Fig. 1G). In the surface vasculature, blood enters through the nasal vessel and leaves the eye through the ventral and dorsal vessels (Fig. 1F, yellow arrows).

## 2.2. Small molecule screen

Previous pharmacological screens in zebrafish identified small molecules affecting development, regeneration, and metabolism (Mathew et al., 2007; Peterson and Fishman, 2004; Peterson et al., 2004; Yu et al., 2008). This approach has not been used, however, to screen for compounds affecting the retina. To develop standard assay conditions for a small molecule screen on the zebrafish retina, we used the *fli1*:EGFP transgenic line to identify compounds affecting the zebrafish retinal vasculature. Around 2000 small molecules from The Spectrum library (Microsource Discovery Systems Inc.) were used to treat embryos at the pectoral fin stage. Embryos were screened for changes in the appearance of retinal blood vessels at several stages, ranging from 3 to 6 dpf. At the concentration tested, 20 compounds resulted in embryonic lethality, 41 caused a loss of EGFP expression but did not affect blood flow, and 10 compounds induced an abnormal morphology in the retinal vasculature. Following a rescreen of these 10 compounds, 5 were found to result in reproducible phenotypes largely specific to the retina, ranging from a widening and fusion of vessels to a nearly complete loss of retinal vasculature (Fig. 3). To determine whether these defects are related to changes in the neural retina, we analyzed the architecture of retinae treated with these compounds on histological sections. One of the 5 compounds produced a severe disorganization of the retina at all concentrations tested, another one produced changes at higher concentrations only, and the remaining 3 did not affect the organization of the retinal layering at all concentrations analyzed (Fig. 4C). For all 5 compounds, following exposure at ca. 2.5 hpf, we identified a range of concentrations that cause vasculature defects in the retina but not in the trunk (Fig. 3, Table 1), indicating a degree of specificity.

The 5 compounds that reproducibly affect the retinal vasculature are: enalapril maleate, pyrogallin, albendazole, mebendazole and zearalenone (Fig. 3). Enalapril maleate and zearalenone produce an increase in the diameter of early ocular vessels, but do not obviously reduce the number of vessels (Fig. 4A). Pyrogallin also causes an increase in the diameter of vessels but in addition it produces a reduction of blood vessel number by ca. 50%. Finally, albendazole and mebendazole dramatically reduce the number of vessels by over 80%. Both compounds occasionally also produce an increase in the diameter of the few vessels that remain intact in the treated retinae (Fig. 4A). Intraocular blood flow stops following exposure to albendazole and mebendazole, while blood flow in the trunk and tail is not affected.

To determine whether eye-specific effects of the above 5 compounds are due to the fact that trunk vessels are more mature and hence more stable at the pectoral fin stage (2.5 dpf), we used these compounds to treated embryos from the 20-somite stage to ca. 2.5 dpf, a developmental period characterized by a rapid expansion of the intersegmental vasculature (Isogai et al., 2003). This is hereafter referred to as the early treatment, while compound addition at 2.5 dpf is referred to as the late treatment. The effect on trunk intersegmental vessels varies depending on the compound used. Enalapril maleate, zearalenone, and pyrogallin do not produce defects in the trunk vasculature at concentrations that cause retina-specific changes following the late treatment (Table 1). Albendazole and mebendazole are more toxic following the early treatment, compared to the late treatment. We did, however, identify one concentration of albendazole that does not produce changes in the trunk vasculature following an early treatment, although it affects eye vasculature following the late one. Finally, mebendazole produces at least a partial vessel loss at all concentrations tested. These results indicate that in general the early trunk vasculature is more sensitive to pharmacological treatment. In the case

of one compound, mebendazole, its strong effect on the eye but not the trunk vasculature following the late treatment may be due to a relative immaturity of eye vessels at this stage. Alternatively, retinal blood vessel defect may be secondary to a general loss of neuronal architecture in the eye.

Enalapril maleate is an angiotensin converting enzyme (ACE) inhibitor, which prevents the synthesis of angiotensin II (Davies et al., 1984; Patchett et al., 1980). This compound is used to treat high blood pressure, heart and renal abnormalities (Bicket, 2002). Enalapril acts on blood vessels and relaxes them, thereby reducing blood pressure (Bicket, 2002). In zebrafish, this compound is toxic at higher concentrations and causes embryonic lethality (Table 1). At lower concentrations, it causes a widening of intraocular blood vessels (Fig. 3, 4 and Table 1), while vessel thickness in the trunk does not display this effect even following an early treatment at the 20-somite stage. To test whether enalapril maleate activity in zebrafish is mediated via the inhibition of ACE, we performed morpholino knockdown of the ACE gene. This experiment did not result in any obvious changes of blood vessel morphology in the eye, possibly due to an incomplete inhibition of the ACE expression (Fig. S1). Alternatively, enalapril maleate acts through an ACE-independent mechanism in retinal vasculature.

Zearalenone, a mycotoxin, also causes an increase of intraocular vessel diameter. Zearalenone and its derivatives display estrogenic activity as they bind to estrogen receptors (Zinedine et al., 2007). In zebrafish, exposure to zearalenone increases vessel diameter in the intraocular vasculature (Table 1). The trunk vasculature remains, however, unaffected following treatments both at 20 somites and at 2.5 dpf (Fig. 3, 4, Table 1, and data not shown). Exposure to higher doses of zearalenone is toxic to embryos (Table 1). Staining with an antibody to phosphorylated histone H3, an indicator of cell proliferation (Pujic and Malicki, 2001), does not reveal obvious changes in cell proliferation patterns, suggesting that other mechanisms are responsible for the change in blood vessel diameter (data not shown).

In contrast to the two compounds discussed above, pyrogallin, promotes loss of about half of retinal blood vessels (Fig. 3, 4A). Vessels that persist frequently cluster together (Fig. 3). Again in the case of this compound, higher doses are toxic to embryos (Table 1). At lower doses, only intraocular vessels seem to be altered as trunk vessel diameter remains normal following chemical treatment at 2.5 dpf (Fig. 3, 4B). A treatment at the 20 somite stage causes either an absence or a delay of trunk vessel formation at higher concentrations of the chemical. The lowest concentration that produces eye vasculature defects (Table 1), does not, however, affect the trunk vasculature even following the early treatment. Fusion of vessels is sometimes produced by enalapril maleate, but this phenotype appears to be more frequent in pyrogallin treated retinæ.

Finally, albendazole and mebendazole are structurally-related, broad spectrum antihelminthic compounds and have been shown to inhibit fumarate reductase, a helminth-specific enzyme (Barrowman et al., 1984; Morgan et al., 1993; Venkatesan, 1998). They have been shown to bind to colchicine sensitive sites of tubulin and inhibit its assembly into microtubules (Morgan et al., 1993). Both albendazole and mebendazole block the uptake of glucose in nematodes (Venkatesan, 1998). At the dose of 0.12 $\times$  albendazole is inactive (data not shown), but at twice this concentration it causes blood vessel defects in the retina but not in the trunk (Table 1). At this concentration, trunk vasculature defects are not observed even following a treatment at 20 somites. Following albendazole treatment, ocular blood vessels collapse, their tissue forms disorderly lumps, and in some cases it is absent altogether (Fig. 3, 4 and Table 1). Mebendazole induces similar phenotypic changes: it causes a drastic reduction or the absence of the vasculature in the retina (Fig. 3, 4). As stated above, however, mebendazole adversely affects the organization of retinal layers, and thus it is possible that the vasculature defect that it induces is secondary. Mebendazole treatment at 2.5 dpf produces a vessel loss in the eye but not in the

trunk at two concentrations tested (Table 1). Both of these concentrations, however, disrupt the trunk vasculature when applied at the 20 somite stage. In contrast to the other three compounds, albendazole and mebendazole predominantly produce a loss of vessels. In some cases vessels appear entirely absent, although in most retinæ, GFP-positive strands and clusters of cells persist, most likely a remnant of vasculature. Given its retinal and trunk vasculature phenotypes, mebendazole is the least specific and appears to display toxicity in many tissues.

Albendazole and mebendazole produce similar phenotypic changes in the zebrafish embryo and are structurally related. Both are very potent at inducing blood vessel loss. The toxicity of mebendazole is a serious disadvantage as it reduces the therapeutic potential of this compound. In an effort to separate toxicity from the ability to induce vessel loss, we searched for additional structurally related compounds. Chemicals that share structural similarity with these two compounds were identified in the small molecule database available on-line at [www.hit2lead.com](http://www.hit2lead.com). This database contains a collection of around 700,000 small molecules distributed commercially and used for biological screening. Searching of this database resulted in the identification of 8 compounds, 5 of which were tested on zebrafish embryos. The five compounds are: methyl{5-chloro-6-[(1-chloro-2-naphthyl)oxy]-1H-benzimidazol-2-yl} carbamate (**MCBC**), methyl[5-(2-thienylcarbonyl)-1H-benzimidazol-2-yl]carbamate (**MBC**), methyl{6-chloro-5-[(4-chloro-1-naphthyl)oxy]-1H-benzimidazol-2-yl}carbamate (**MCNBC**), butyl 2-({2-[(methoxycarbonyl)amino]-1H-benzimidazol-5-yl}carbonyl) benzoate (**BBC**), and ethyl 1H-benzimidazol-2-ylcarbamate (**EBC**) (Fig. 5). For simplicity, we will refer to these chemicals using abbreviations provided in parentheses above. Four out of the 5 compounds produce phenotypes that at least at some concentrations are specific to the intraocular vasculature following the late treatment (Table 2). Similar to albendazole and mebendazole, these chemicals produce a reduction in the number of intraocular blood vessels. The strength of phenotypic changes induced by these compounds at the highest specific concentration tested is quantitated in Fig 5: while MCNBC and EBC produce the complete absence of retinal vessels, MCBC and BBC treatment results only a partial vessel loss (Fig. 5, Table 2). The fifth compound, MBC, appears to be extremely potent, and even at very high dilutions causes a complete vessel loss in the eye. MBC lacks specificity, however, as even at the lowest effective concentration it affects both eye and trunk vessels. It is lethal to the embryo at nearly all concentrations that produce eye vasculature defects (Table 2). At the dilution of 0.05× (data not shown), MBC does not produce any obvious phenotypic changes. These 5 compounds display varying impact on the organization of retinal neurons (Fig. 5 and Table 2). MBC causes a severe disorganization of retinal architecture at all effective concentrations (Fig. 5), indicating a lack of specificity, MCNBC and EBC cause a partial disruption of retinal layers, and, finally, BBC and MCBC do not affect the retinal architecture in any obvious way.

### 3. Discussion

One attractive feature of the zebrafish retina is its potential use as a model of events that occur in human eye development. It is thus important to determine whether zebrafish vasculature is morphologically related to the human one. Indeed, our studies indicate that some morphological and developmental characteristics of zebrafish retinal vasculature are similar to those in primates. Others, however, differ. The arrangement of early retinal vessels in zebrafish, for example, is similar to that of the hyaloid vasculature of the human embryo, where it has been compared to strings of an open parachute (Mutlu and Leopold, 1964; Zhu et al., 1999). A major difference between the zebrafish and primates, on the other hand, is a complete regression of the hyaloid vasculature by the time of birth in the latter group of animals (Fruttiger, 2002; Dorrell, 2002). The transition from embryonic to mature vasculature in zebrafish is much less dramatic, and involves a gradual change in the adhesive properties of blood vessels, which at the onset of their development adhere to the lens (Fig. 1D–L and Fig. 2 A–D, F–G) and by 30 dpf are associated with the inner surface of the retina (Alvarez et al.,

2007, and Fig. 1N). Another obvious difference between zebrafish and mammals is the absence of the secondary vessel plexus, which penetrates neuronal formations of primate retinae (Provis, 2001). One has to note, however, that the pattern of blood vessels varies greatly even among mammals: while primates feature retinae entirely covered by a network of blood vessels, marsupial retinae are avascular (Wise et al., 1971).

Angiogenesis in the retina is a very carefully regulated process. Both an overproduction of blood vessels as well as their deficiency lead to eye disease. We identified at least two categories of chemicals that affect retinal vasculature: compounds that cause a collapse and a loss of vessels as well as compounds that cause a widening of vessel diameter. These compounds may help to understand mechanisms that underlie the formation and patterning of blood vessels, and each of these two categories can be potentially applied to alleviate the symptoms of a different class of human diseases. For example, persistent fetal vasculature is a human abnormality that involves a loss or a slowdown of hyaloid vasculature regression (Goldberg, 1997). One can thus imagine that albendazole or related chemicals could be used to induce a degeneration of these vessels in children affected by this abnormality. Similarly, one can imagine that this class of compounds could be used to slow down the progression of ocular tumors. Zearalenone, on the other hand, appears to increase the diameter of blood vessels but does not cause changes in their number, and thus could be used to treat different forms of retinal blood vessel occlusion. Branch retinal vein occlusion, the second most common vascular abnormality in the retina, is one example of a disease that could be alleviated by inducing an increase of blood vessel diameter (McIntosh et al., 2007). Importantly, when tested in zebrafish, albendazole and zearalenone appear to be more potent in the retina, compared to vessels in other organs. This characteristic is desirable for chemicals that can be potentially applied to treat eye disease.

Small molecule screens frequently result in the identification of compounds that produce a loss of tissue phenotype. This is often due to their toxicity or the propensity to cause a developmental delay. In the screen presented here, we have found both chemicals that cause vessel loss, and compounds that enhance the wild-type phenotype: increase blood vessel diameter. The mode of action of chemicals that cause a gain of a phenotypic feature is frequently more specific, and tends to be relevant to developmental or physiological processes confined to an organ or tissue. Indeed, the phenotypes of the compounds that increase blood vessel diameter, Enalapril Maleate, and Zearalenone, appear confined to the ocular vasculature as they do not disrupt retinal architecture in any obvious way. Likewise, they do not affect the trunk vasculature even following a treatment at the 20-somite stage. In contrast to that, 2 of the 3 compounds that cause blood vessel loss also affect the organization of retinal neurons. In the case of one chemical, mebendazole, vascular and neuronal phenotypes cannot be easily separated by varying its concentration. This is a negative factor that reduces therapeutic potential of mebendazole.

Although the strength of mebendazole-induced blood vessel loss is impressive, the therapeutic potential of this compound is negatively impacted by the lack of specificity. In an effort to reduce toxicity while preserving retina-specific blood vessel activity, we tested 5 compounds related to albendazole and mebendazole (Fig. 5). Ethyl 1H-benzimidazol-2-ylcarbamate (EBC) is the moiety shared by albendazole, mebendazole, and all other compounds tested. This moiety alone is sufficient to produce a retina-specific vascular phenotype, although its potency is lower, compared to the two original isolates (Table 2). The difference in potency between EBC and albendazole is seen in the minimum amount needed to affect retinal blood vessels (Table 1 and 2). In excess of 10-fold higher molar concentration of EBC is required to induce an eye phenotype, compared to albendazole. On the basis of this parameter, the addition of methyl N-propyl sulphide group to the EBC moiety (as seen in albendazole) and the addition of an acetophenone group (as seen in mebendazole) both result in an increased potency. If one defines

specificity as the strongest retinal phenotype that is not accompanied by trunk vasculature defects, EBC and albendazole display similar specificity as they both cause a complete or a nearly-complete elimination of blood vessels in the retina, without affecting the trunk vasculature (Fig. 5). Albendazole, however, appears to be more specific when one considers retinal architecture: at all effective concentrations, EBC causes at least a partial disorganization of retinal neurons. Other EBC modifications seem to decrease specificity, compared to albendazole. While BBC and MCBC do not affect the organization of retinal neurons, they display lower specificity as defined above. MCB and MCNBC, on the other hand, cause a disorganization of retinal architecture. The addition of 2-acetylthiophene group in MBC causes a dramatic increase in potency but severely eliminates specificity: even at the lowest effective concentration tested (X in Table 2), MBC phenotype affects both retinal and trunk vessels (Table 2, and data not shown). The toxicity of this compound is also much higher as evaluated by the overall lethality of embryos, compared to other chemicals tested.

Once promising chemicals are identified, a major challenge is to determine their mode of action. Several strategies can be used to accomplish this goal. In some cases, the phenotype resulting from a chemical treatment is informative enough to suggest candidate molecular pathways that may be affected (Sachidanandan et al., 2008). When this is not a possible, a variety of biochemical approaches are available, including affinity purification, the use of protein microarrays, cell microarrays, and phage display (reviewed in Sleno and Emili, 2008; Terstappen et al., 2007). Affinity purification is one option that has been frequently used for the purification of target proteins from cultured cells or animal tissues (Bach et al., 2005; Tanaka et al., 2005). This method can be easily adapted to extracts from whole zebrafish embryos or from specific adult tissues, such as the eye.

Small-molecule screening is a powerful approach to drug discovery. A combination of this approach with genomic studies, so-called chemogenomics, promises to be even more productive (Agrafiotis et al., 2002). The use of zebrafish in this dynamic field provides an additional exciting dimension, as it allows one for an inexpensive high-throughput testing of chemicals in the context of an intact organism. In this study, we explore a specific application of this approach to the retinal vasculature. To our knowledge, an assay of this kind has not been available so far. Our results suggest that this type of analysis can indeed become an important addition to the existing genetic, cell biological, and biochemical methodologies.

## 4. Experimental procedures

### 4.1. Zebrafish strains

Zebrafish were raised on 14/10 hour light cycle. Embryos were obtained via natural mating, and staged according to Kimmel et al. (Kimmel et al., 1995). Embryos older than 24 hpf were treated with 0.03% Phenylthiourea (PTU) to block pigmentation. Transgenic fish expressing EGFP under the control of *fli1* (*Tg(fli1:EGFP)*) were obtained from zebrafish resource center (Oregon, USA). The *Tg(flk1:GFP)* line was provided by Zygogen Inc. (Atlanta, Georgia, USA).

### 4.2. Imaging of zebrafish vasculature and image analysis

To study wild-type development of the ocular vasculature, transgenic zebrafish embryos were anesthetized with 0.1% Tricane, and transferred onto a 1% Agarose bed in a Petri dish. A few drops of 1% low melting point agarose were laid over each embryo and embryos was immediately oriented as appropriate on the dorsal, ventral or lateral side. After agarose solidified, 5 – 10 ml of egg water with 0.03% PTU was added to the Petri dish. The vasculature of embedded embryos was then reconstructed using a Leica SP2 confocal microscope equipped



with a 40× water immersion lens. Images were collected and processed with ImageJ and Adobe Photoshop Software.

To reveal details of wild-type vascular architecture, embryos were fixed in 4% paraformaldehyde in PBST (phosphate buffered saline, 0.1% Tween) for 2 hrs, washed 2 times, 5 min. each, in PBST, and infiltrated with a medium containing equal amounts of 30% sucrose and Neg-50 frozen section medium (Richard-Allen Scientific) overnight at 4°C. Subsequently, embryos were embedded in neg-50 frozen section medium and 12 μm of sections were collected. Sections were dried at room temperature for 30 min., washed 2 times, 5min each, in PBST, coverslipped, and imaged using Leica SP2 confocal microscope equipped with a 40× lens. Digital images were processed with Adobe Photoshop Software.

To generate movies showing blood circulation in the retina, embryos were incubated in egg water containing 0.03% PTU until 72 hpf, transferred onto a 1% Agarose bed, immobilized as above, and oriented either lateral side up (to image surface circulation) or ventral side up (to image early ocular circulation). Blood circulation was recorded using a Leica SP2 confocal microscope and Leica imaging software. The data were then exported at 5 frames per second into AVI movie format.

To screen for effects of small molecules on the retinal vasculature, embryos were anesthetized with 0.1% Tricane and transferred to depression glass slide filled with methyl cellulose. Embryos were positioned on their sides and examined using a Zeiss Axiovert 200 inverted microscope equipped with a 10× lens. Images of embryos were acquired with a cooled CCD camera (Princeton Instrument MicroMAX) operated by LabView Software package (National Instruments, Austin, TX), and processed using Adobe Photoshop Software. To evaluate the number of blood vessels per retina, we counted the number of vessel segments that met the following criteria: were characterized by roughly parallel walls, displayed distinct lumen, were open at both ends, and stretched for a minimum of 15 arbitrary length units (measured in pixels on Photoshop images). The results of these counts are provided in Fig. 4. Clumps of GFP-positive tissue that did not have a lumen or were not open at both ends were considered “collapsed vessels” and were not counted. To compare the width of vessels in wild-type and chemically-treated retinæ, the diameter of the widest vessel segment as defined above was measured from each retina. A line along the long axis of this segment was drawn (such as yellow lines in Fig. 3A) and the inner diameter was measured in its widest portion (other than widening of its ends) by drawing a line perpendicular to segment’s long axis (red line in Fig. 3).

### 4.3. Small molecule screen

Two thousand compounds from the Spectrum Collection (Microsource Discovery Systems Inc.) of small molecules were screened on zebrafish embryos placed in 96-well clear bottom plates (Corning Inc.) in egg water containing PTU. Before screen compounds were added, medium was replaced with 200ul of fresh PTU-containing egg water. Since the small molecules were dissolved in DMSO, a series of DMSO concentrations was tested for the ability of affect zebrafish embryogenesis. As  $\geq 6\mu\text{l}$  of DMSO in 200μl of egg water is toxic to embryos, 2μl or less was used in our experiments. Two variants of the screen were performed. In the first variant, embryos were kept at the room temperature for the first 24 hours (ca. until the 20 somite stage), and for each chemical tested ca. 100 nl of stock solution (10mM in DMSO) were added by pin transfer. Embryos were then transferred to 28°C and their development was periodically documented directly in 96-well plates at 24, 48, and 72 hpf using a 10× lens on a Zeiss Axiovert 200 Inverted microscope. In the second variant of the screen, embryos were also transferred to 28°C after 24 hours of development at the room temperature, but chemicals were added at 68 hours after fertilization. Given the delay caused by storage at room temperature during the

first 24 hours of development, this corresponds to ca. pectoral fin stage. The phenotype was periodically documented at 72, 96, 120, and 144 hpf as described above.

The first variant of the screen produced very high lethality and no compounds of interest were identified. The second variant resulted in the identification of 5 compounds that produce specific phenotypic changes in the eye vasculature. Chemicals that produced phenotypic changes in the initial rounds of screening were purchased in a larger quantity, and 10 mg of each was dissolved in 2ml of DMSO. To determine the minimum amount of each compound sufficient to produce a phenotype, a series of dilutions was prepared in egg water containing PTU (Table 1). These dilutions were tested on embryos as described above.

As two related chemicals, albendazole and mebendazole, produced similar phenotypes, we decided to test other compounds structurally related to these two. The region shared between albendazole and mebendazole was used to search a database of available chemicals (www.hit2lead.com). This search resulted in the identification of 8 compounds, which contain the substructure shared between albendazole and mebendazole. Out of these, 5 compounds were selected for further testing, based on differences from the query structure. 5 mg of each were obtained from ChemBridge corporation and dissolved in 1ml of DMSO. This stock solution was diluted by adding 4, 3, 2, 1, 0.5, or 0.25 $\mu$ l to 200 $\mu$ l of with egg water and tested for phenotypic effects on embryos. Phenotypic changes were monitored and recorded as above (Table 2).

#### 4.4 Morpholino knockdown

Antisense knockdowns were performed using standard protocols, as described previously using either 5  $\mu$ g/ $\mu$ l or 9  $\mu$ g/ $\mu$ l of CATTGATATGATTCATGTACCTGAA splice-site directed morpholino. Knockdown efficiency was monitored via RT-PCR as described previously (Tsujikawa and Malicki, 2004), using the primers TTAAAGGTCCCATCCCTGCTCATC and TTAAAGGTCCCATCCCTGCTCATC.

### Supplementary Material

Refer to Web version on PubMed Central for supplementary material.

### Acknowledgments

We would like to thank Dr. William F. Sewell from the Department of Otolaryngology at Harvard Medical School for providing access to an inverted microscope, Dr. Chengtian Zhao for help with designing anti-ACE morpholino, Drs. Agneta Mode, Arindam Majumdar, and Breandan Kennedy for comments on earlier versions of this manuscript, Drs. Jan Åke Gustafsson, Agneta Mode, Lotta Hambræus, Sodertorns Hogskola, and Department of Biosciences and Medical Nutrition at Karolinska Institutet for funding and support. Drs. Peter Schuller, Amy Doherty, and David Kokel from Randall Peterson lab as well as Dr. Caroline Shamu of the Institute of Chemistry and Cell Biology at Harvard Medical School provided valuable technical advice during this work. This project was funded in part by a National Eye Institute award RO1 EY016859 (to JM).

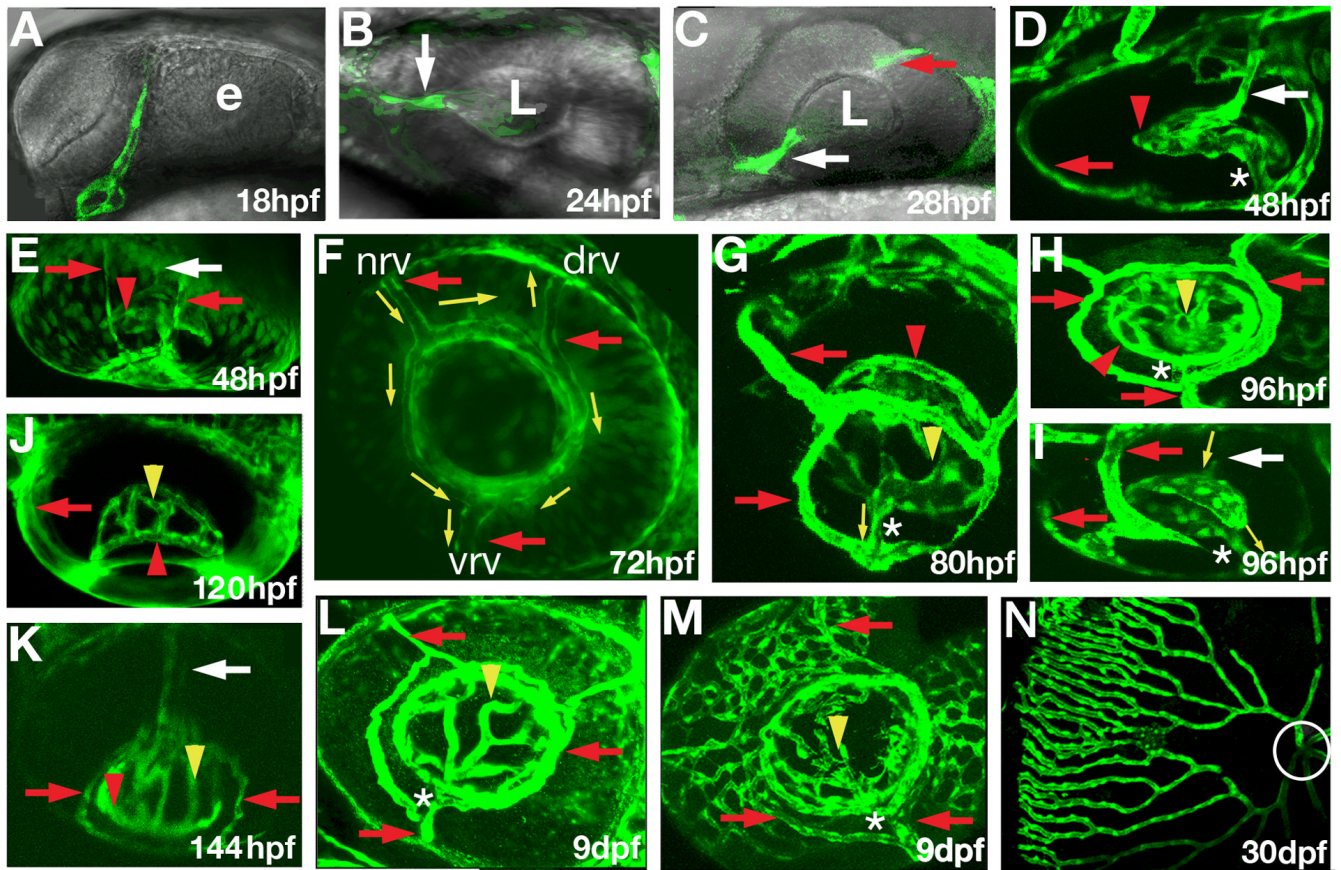
### References

- Agrafiotis DK, Lobanov VS, Salemme FR. Combinatorial informatics in the post-genomics ERA. *Nat Rev Drug Discov* 2002;1:337–46. [PubMed: 12120409]
- Alvarez Y, Cederlund ML, Cottell DC, Bill BR, Ekker SC, Torres-Vazquez J, Weinstein BM, Hyde DR, Vihtelic TS, Kennedy BN. Genetic determinants of hyaloid and retinal vasculature in zebrafish. *BMC Dev Biol* 2007;7:114. [PubMed: 17937808]
- Amsterdam A, Nissen RM, Sun Z, Swindell EC, Farrington S, Hopkins N. Identification of 315 genes essential for early zebrafish development. *Proc Natl Acad Sci U S A* 2004;101:12792–7. [PubMed: 15256591]

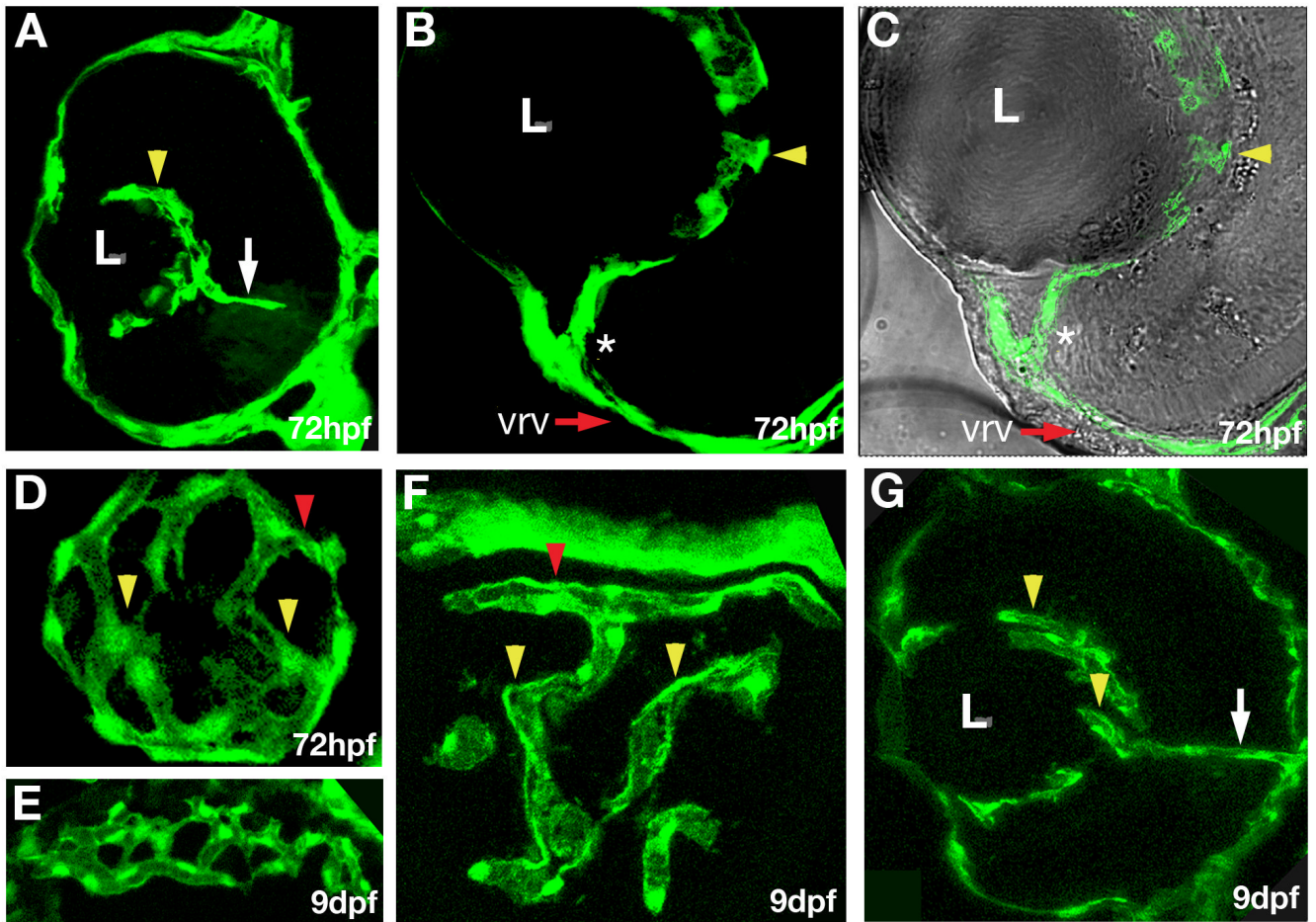
- Avanesov A, Malicki J. Approaches to study neurogenesis in the zebrafish retina. *Methods Cell Biol* 2004;76:333–84. [PubMed: 15602883]
- Bach S, Knockaert M, Reinhardt J, Lozach O, Schmitt S, Baratte B, Koken M, Coburn SP, Tang L, Jiang T, Liang DC, Galons H, Dierick JF, Pinna LA, Meggio F, Totzke F, Schachtele C, Lerman AS, Carnero A, Wan Y, Gray N, Meijer L. Roscovitine targets, protein kinases and pyridoxal kinase. *J Biol Chem* 2005;280:31208–19. [PubMed: 15975926]
- Barrowman MM, Marriner SE, Bogan JA. The fumarate reductase system as a site of anthelmintic attack in *Ascaris suum*. *Biosci Rep* 1984;4:879–83. [PubMed: 6518278]
- Bicket DP. Using ACE inhibitors appropriately. *Am Fam Physician* 2002;66:461–8. [PubMed: 12182524]
- Choi J, Dong L, Ahn J, Dao D, Hammerschmidt M, Chen JN. FoxH1 negatively modulates flk1 gene expression and vascular formation in zebrafish. *Dev Biol* 2007;304:735–44. [PubMed: 17306248]
- Davies RO, Gomez HJ, Irvin JD, Walker JF. An overview of the clinical pharmacology of enalapril. *Br J Clin Pharmacol* 1984;18(Suppl 2):215S–229S. [PubMed: 6099737]
- Driever W, Solnica-Krezel L, Schier AF, Neuhauss SC, Malicki J, Stemple DL, Stainier DY, Zwartkruis F, Abdelilah S, Rangini Z, Belak J, Boggs C. A genetic screen for mutations affecting embryogenesis in zebrafish. *Development* 1996;123:37–46. [PubMed: 9007227]
- Easter S, Nicola G. The development of vision in the zebrafish (*Danio rerio*). *Dev Biol* 1996;180:646–663. [PubMed: 8954734]
- Goldberg MF. Persistent fetal vasculature (PFV): an integrated interpretation of signs and symptoms associated with persistent hyperplastic primary vitreous (PHPV). LIV Edward Jackson Memorial Lecture. *Am J Ophthalmol* 1997;124:587–626. [PubMed: 9372715]
- Grunwald JE, Hariprasad SM, DuPont J, Maguire MG, Fine SL, Brucker AJ, Maguire AM, Ho AC. Foveolar choroidal blood flow in age-related macular degeneration. *Invest Ophthalmol Vis Sci* 1998;39:385–90. [PubMed: 9477998]
- Haffter P, Granato M, Brand M, Mullins MC, Hammerschmidt M, Kane DA, Odenthal J, van Eeden FJ, Jiang YJ, Heisenberg CP, Kelsh RN, Furutani-Seiki M, Vogelsang E, Beuchle D, Schach U, Fabian C, Nusslein-Volhard C. The identification of genes with unique and essential functions in the development of the zebrafish, *Danio rerio*. *Development* 1996;123:1–36. [PubMed: 9007226]
- Hu M, Easter SS. Retinal neurogenesis: the formation of the initial central patch of postmitotic cells. *Dev Biol* 1999;207:309–321. [PubMed: 10068465]
- Isogai S, Lawson ND, Torrealday S, Horiguchi M, Weinstein BM. Angiogenic network formation in the developing vertebrate trunk. *Development* 2003;130:5281–90. [PubMed: 12954720]
- Kato M, Patel MS, Levasseur R, Lobov I, Chang BH, Glass DA 2nd, Hartmann C, Li L, Hwang TH, Brayton CF, Lang RA, Karsenty G, Chan L. Cbfa1-independent decrease in osteoblast proliferation, osteopenia, and persistent embryonic eye vascularization in mice deficient in Lrp5, a Wnt coreceptor. *J Cell Biol* 2002;157:303–14. [PubMed: 11956231]
- Killingsworth MC, Sarks JP, Sarks SH. Macrophages related to Bruch's membrane in age-related macular degeneration. *Eye* 1990;4(Pt 4):613–21. [PubMed: 2226993]
- Kimmel CB, Ballard WW, Kimmel SR, Ullmann B, Schilling TF. Stages of embryonic development of the zebrafish. *Dev Dyn* 1995;203:253–310. [PubMed: 8589427]
- Lang RA, Bishop JM. Macrophages are required for cell death and tissue remodeling in the developing mouse eye. *Cell* 1993;74:453–62. [PubMed: 8348612]
- Lawson ND, Weinstein BM. In vivo imaging of embryonic vascular development using transgenic zebrafish. *Dev Biol* 2002;248:307–18. [PubMed: 12167406]
- Lobov IB, Rao S, Carroll TJ, Vallance JE, Ito M, Ondr JK, Kurup S, Glass DA, Patel MS, Shu W, Morrissey EE, McMahon AP, Karsenty G, Lang RA. WNT7b mediates macrophage-induced programmed cell death in patterning of the vasculature. *Nature* 2005;437:417–21. [PubMed: 16163358]
- Mathew LK, Sengupta S, Kawakami A, Andreasen EA, Lohr CV, Loynes CA, Renshaw SA, Peterson RT, Tanguay RL. Unraveling tissue regeneration pathways using chemical genetics. *J Biol Chem* 2007;282:35202–10. [PubMed: 17848559]
- McIntosh RL, Mohamed Q, Saw SM, Wong TY. Interventions for branch retinal vein occlusion: an evidence-based systematic review. *Ophthalmology* 2007;114:835–54. [PubMed: 17397923]

- Melet F, Motro B, Rossi DJ, Zhang L, Bernstein A. Generation of a novel Fli-1 protein by gene targeting leads to a defect in thymus development and a delay in Friend virus-induced erythroleukemia. *Mol Cell Biol* 1996;16:2708–18. [PubMed: 8649378]
- Meyer D, Wolff CM, Stiegler P, Senan F, Befort N, Befort JJ, Remy P. Xl-fli, the *Xenopus* homologue of the fli-1 gene, is expressed during embryogenesis in a restricted pattern evocative of neural crest cell distribution. *Mech Dev* 1993;44:109–21. [PubMed: 8155576]
- Morgan UM, Reynoldson JA, Thompson RC. Activities of several benzimidazoles and tubulin inhibitors against *Giardia* spp. in vitro. *Antimicrob Agents Chemother* 1993;37:328–31. [PubMed: 8452365]
- Mutlu F, Leopold IH. The Structure of Fetal Hyaloid System and Tunica Vasculosa Lentis. *Arch Ophthalmol* 1964;71:102–10. [PubMed: 14066026]
- Nasevicius A, Ekker SC. Effective targeted gene ‘knockdown’ in zebrafish. *Nat Genet* 2000;26:216–220. [PubMed: 11017081]
- Nawrocki, W. PhD Thesis Thesis. University of Oregon; Eugene, Oregon: 1985. Development of the neural retina in the zebrafish, *Brachydanio rerio*.
- North TE, Goessling W, Walkley CR, Lengerke C, Kopani KR, Lord AM, Weber GJ, Bowman TV, Jang IH, Grosser T, Fitzgerald GA, Daley GQ, Orkin SH, Zon LI. Prostaglandin E2 regulates vertebrate haematopoietic stem cell homeostasis. *Nature* 2007;447:1007–11. [PubMed: 17581586]
- Patchett AA, Harris E, Tristram EW, Wyvrat MJ, Wu MT, Taub D, Peterson ER, Ikeler TJ, ten Broeke J, Payne LG, Ondeyka DL, Thorsett ED, Greenlee WJ, Lohr NS, Hoffsommer RD, Joshua H, Ruyle WV, Rothrock JW, Aster SD, Maycock AL, Robinson FM, Hirschmann R, Sweet CS, Ulm EH, Gross DM, Vassil TC, Stone CA. A new class of angiotensin-converting enzyme inhibitors. *Nature* 1980;288:280–3. [PubMed: 6253826]
- Peterson RT, Fishman MC. Discovery and use of small molecules for probing biological processes in zebrafish. *Methods Cell Biol* 2004;76:569–91. [PubMed: 15602893]
- Peterson RT, Link BA, Dowling JE, Schreiber SL. Small molecule developmental screens reveal the logic and timing of vertebrate development. *Proc Natl Acad Sci U S A* 2000;97:12965–9. [PubMed: 11087852]
- Peterson RT, Shaw SY, Peterson TA, Milan DJ, Zhong TP, Schreiber SL, MacRae CA, Fishman MC. Chemical suppression of a genetic mutation in a zebrafish model of aortic coarctation. *Nat Biotechnol* 2004;22:595–9. [PubMed: 15097998]
- Provis JM. Development of the primate retinal vasculature. *Prog Retin Eye Res* 2001;20:799–821. [PubMed: 11587918]
- Pujic Z, Malicki J. Mutation of the zebrafish glass onion locus causes early cell-nonautonomous loss of neuroepithelial integrity followed by severe neuronal patterning defects in the retina. *Developmental Biology* 2001;234:454–69. [PubMed: 11397013]
- Ross RD, Barofsky JM, Cohen G, Baber WB, Palao SW, Gitter KA. Presumed macular choroidal watershed vascular filling, choroidal neovascularization, and systemic vascular disease in patients with age-related macular degeneration. *Am J Ophthalmol* 1998;125:71–80. [PubMed: 9437316]
- Sachidanandan C, Yeh J, Peterson Q, Peterson R. Identification of a Novel Retinoid by Small Molecule Screening with Zebrafish Embryos. *PLOS ONE* 2008;3:1–9.
- Saint-Geniez M, D’Amore PA. Development and pathology of the hyaloid, choroidal and retinal vasculature. *Int J Dev Biol* 2004;48:1045–58. [PubMed: 15558494]
- Sleno L, Emili A. Proteomic methods for drug target discovery. *Curr Opin Chem Biol* 2008;12:46–54. [PubMed: 18282485]
- Smith LE. Pathogenesis of retinopathy of prematurity. *Growth Horm IGF Res* 2004;(14 Suppl A):S140–4. [PubMed: 15135797]
- Tanaka M, Bateman R, Rauh D, Vaisberg E, Ramachandani S, Zhang C, Hansen KC, Burlingame AL, Trautman JK, Shokat KM, Adams CL. An unbiased cell morphology-based screen for new, biologically active small molecules. *PLoS Biol* 2005;3:e128. [PubMed: 15799708]
- Terstappen GC, Schlupen C, Raggiaschi R, Gaviraghi G. Target deconvolution strategies in drug discovery. *Nat Rev Drug Discov* 2007;6:891–903. [PubMed: 17917669]
- Thompson MA, Ransom DG, Pratt SJ, MacLennan H, Kieran MW, Detrich HW 3rd, Vail B, Huber TL, Paw B, Brownlie AJ, Oates AC, Fritz A, Gates MA, Amores A, Bahary N, Talbot WS, Her H, Beier

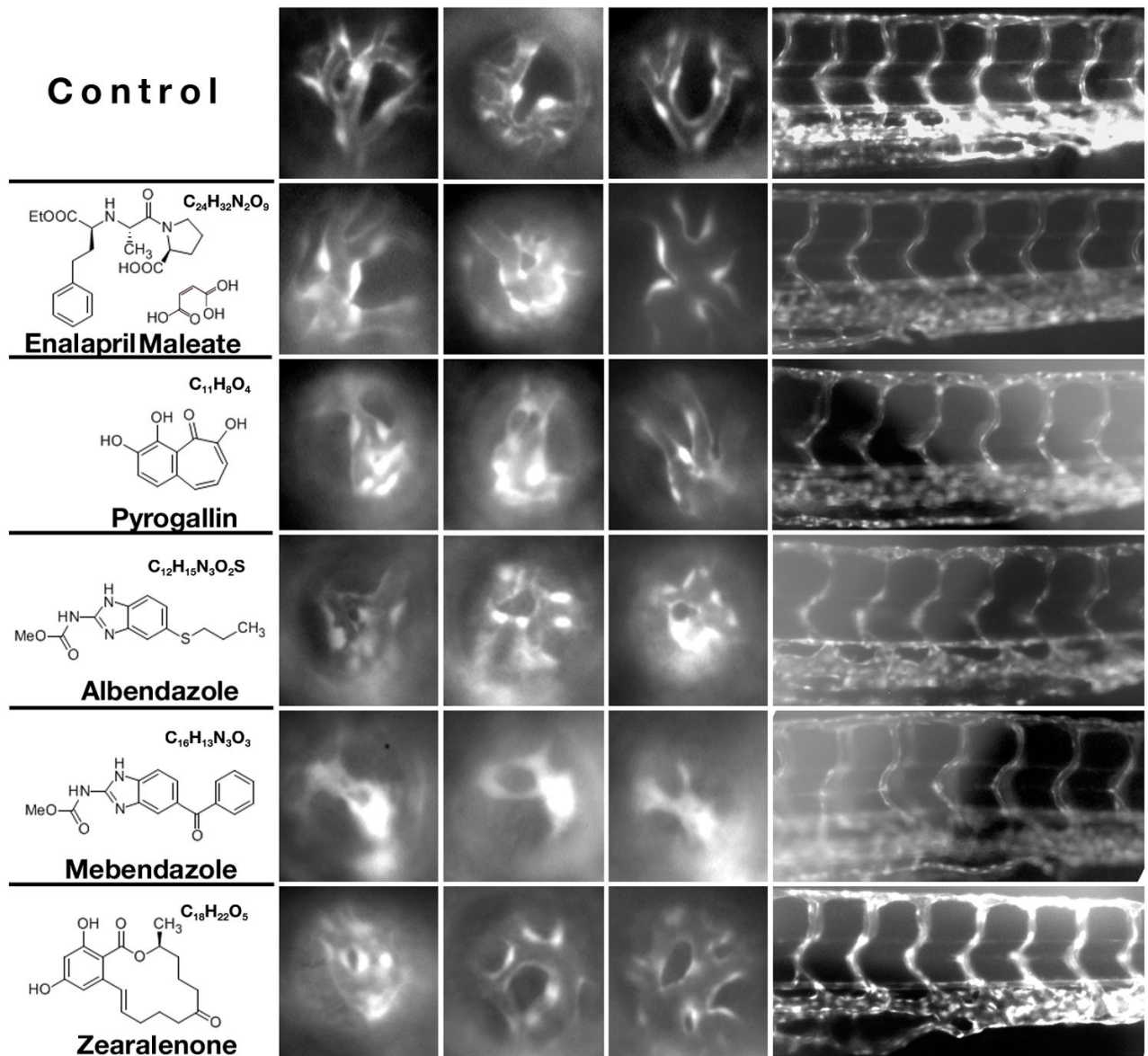
- DR, Postlethwait JH, Zon LI. The cloche and spadetail genes differentially affect hematopoiesis and vasculogenesis. *Dev Biol* 1998;197:248–69. [PubMed: 9630750]
- Tran TC, Sneed B, Haider J, Blavo D, White A, Aiyejorun T, Baranowski TC, Rubinstein AL, Doan TN, Dingleline R, Sandberg EM. Automated, quantitative screening assay for antiangiogenic compounds using transgenic zebrafish. *Cancer Res* 2007;67:11386–92. [PubMed: 18056466]
- Tsujikawa M, Malicki J. Intraflagellar transport genes are essential for differentiation and survival of vertebrate sensory neurons. *Neuron* 2004;42:703–16. [PubMed: 15182712]
- Venkatesan P. Albendazole. *J Antimicrob Chemother* 1998;41:145–7. [PubMed: 9533454]
- Weber BH, Vogt G, Pruett RC, Stohr H, Felbor U. Mutations in the tissue inhibitor of metalloproteinases-3 (TIMP3) in patients with Sorsby's fundus dystrophy. *Nat Genet* 1994;8:352–6. [PubMed: 7894485]
- Wienholds E, Schulte-Merker S, Walderich B, Plasterk RH. Target-selected inactivation of the zebrafish rag1 gene. *Science* 2002;297:99–102. [PubMed: 12098699]
- Wise, G.; Dollery, C.; Henkind, P. *The Retinal Circulation*. Harper & Row; New York: 1971.
- Xu Q, Wang Y, Dabdoub A, Smallwood PM, Williams J, Woods C, Kelley MW, Jiang L, Tasman W, Zhang K, Nathans J. Vascular development in the retina and inner ear: control by Norrin and Frizzled-4, a high-affinity ligand-receptor pair. *Cell* 2004;116:883–95. [PubMed: 15035989]
- Yu PB, Hong CC, Sachidanandan C, Babbitt JL, Deng DY, Hoyng SA, Lin HY, Bloch KD, Peterson RT. Dorsomorphin inhibits BMP signals required for embryogenesis and iron metabolism. *Nat Chem Biol* 2008;4:33–41. [PubMed: 18026094]
- Zhu M, Provis JM, Penfold PL. The human hyaloid system: cellular phenotypes and inter-relationships. *Exp Eye Res* 1999;68:553–63. [PubMed: 10328969]
- Zinedine A, Soriano JM, Molto JC, Manes J. Review on the toxicity, occurrence, metabolism, detoxification, regulations and intake of zearalenone: an oestrogenic mycotoxin. *Food Chem Toxicol* 2007;45:1–18. [PubMed: 17045381]
- Zon LI, Peterson RT. In vivo drug discovery in the zebrafish. *Nat Rev Drug Discov* 2005;4:35–44. [PubMed: 15688071]



**Fig. 1.** Early development of retinal vasculature in zebrafish. Confocal images of GFP expression in the eyes of *fli1:EGFP* (B, E, F, J, K) and *flk1:GFP* (A, C, D, G, H, I, L, M, N) transgenic zebrafish. The retinal artery or its presumptive primordium is indicated by white arrows. Red arrows point to the surface vasculature. Red arrowheads indicate the intraocular ring vessel. Yellow arrowheads indicate the intraocular vessel network, whereas the connection between the intraocular and surface vessels is indicated by asterisks. Yellow arrows show the direction of blood flow. (A) GFP-expressing cells are absent in the eye at 18 hpf. (B) GFP-positive cells are seen in the retina by 24 hpf (B, white arrow). (C) By 28 hpf, GFP-positive cells are seen in the choroid fissure (white arrow), behind the lens, and in the posterior groove (red arrow). (D, E) By 48 hpf, GFP-positive cells form a network of vessels around the medial side of the lens, annular collection duct (asterisk) is established, and surface vessels are differentiated. Retinal blood flow is present by 72 hpf. (F) In the surface vasculature, blood enters through the nasal vessel (nrv) and exits through the dorsal (drv) and ventral (vrv) vessels. (G – I) Blood from the intraocular vasculature flows through the annular collection duct (asterisks) into the surface vessels. (J – K) Intraocular vessels gradually rearrange to form a roughly radial array by 144 hpf. (L) Intraocular and surface vasculatures at 9 dpf. (M) Choroidal vessels form a network on the outer surface of the eye at 9 dpf. (N) The eye vasculature at 30 dpf. Circle indicates the optic disc region. The retina was dissected and mounted on a flat surface to obtain this image. e, optic lobe; L, lens. In (A–M) anterior is left. In (A–C, G, H, L, F, M, and N) dorsal is up. Panels (A, B, C, F, H, L and M) show roughly the lateral view of the eye. Panels (D–E, I, J, and K) show ventral view of the eye.

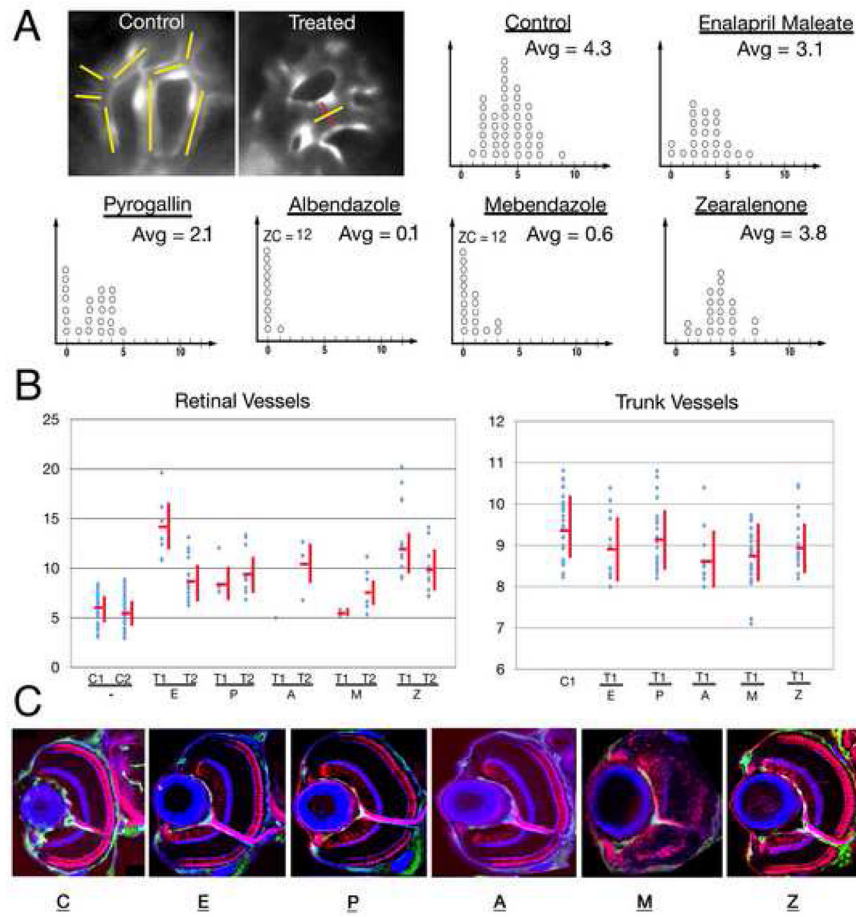


**Fig. 2.** Characterization of early retinal vasculature. Confocal images of cryosections through eyes of *fli1:EGFP* transgenic animals. (A – C) Transverse sections through the retina. Intraocular vessels (yellow arrowheads) wrap around the lens, and are connected to the surface vessel (asterisk) at 72 hpf. Dorsal is up and lateral to the left. (D) A somewhat oblique longitudinal section through the region behind the lens reveals a vessel network on the surface of the lens. Posterior is to the right, lateral is down. (E) A transverse tangential section through the rostral eye showing the chorioidal vessel network at 9 dpf. (F) A transverse section tangential to the lens showing the intraocular ring vessel (red arrowhead) and the intraocular vessel network (yellow arrowheads) at 9 dpf. (G) A transverse section showing intraocular vessels at 9 dpf, dorsal is up, and lateral to the left. The retinal artery is indicated by white arrow.



**Fig. 3.** Phenotypic changes in the retinal vasculature following treatment with different chemicals. Shown are lateral views of the retinal vasculature through the lens at 96 hpf (3 left-most columns of images), as well as lateral views of the trunk vasculature (right-most column of images, dorsal is up). Each row shows three examples of the phenotype induced in the retina and one example of trunk phenotype. Note that in the most extreme cases, vessels are not observed at all and GFP-positive tissue forms irregular clumps. Such clumps of tissue are not counted as vessel segments in graphs presented in Fig. 4. The name, formula, and the structure of each chemical are provided to the left of image panels.



**Fig. 4.**

The number and thickness of retinal and trunk vessels following treatment with different chemicals. (A) Top left image panels illustrate the method of counting and measuring vessels. In the control image panel, yellow lines indicate the vessel segments. The image of a treated retina shows an example of vessel segment thickness measurement (the line in red indicates thickness). Graphs in panel A show the number of ocular vessel segments in control and chemically treated animals. x-axis provides the number of vessel segments per eye; each circle represents a single retina. Retinae with absent or collapsed vessels only are given the value of 0. The average number of blood vessel segments (Avg) per eye is provided in the upper left corner of each graph. In cases where the number of retinae in the zero category exceeds 10, its size is provided numerically as ZC (zero category). In this experiment, for each compound, we chose the highest concentration that is known to produce retinal blood vessel changes but does not affect trunk vasculature (Mebendazole) or retinal lamination (Enalapril Maleate, Pyrogallin, Albendazole, and Zearalenone). (B) Vessel thickness measurements in control and chemically-treated embryos. Untreated controls are indicated as C1 and C2, while small molecule tests as T1 and T2. T1 represents the highest concentration producing eye-specific vasculature phenotype that does not cause a disorganization of the retina and T2 represents the lowest concentration sufficient to produce an eye vasculature phenotype. In the case of mebendazole, neuronal organization is affected at all concentrations tested, and so we provide data for the highest concentration that affects the eye but not the trunk vasculature. Statistically significant values were obtained for T1 and T2 concentrations of each compound with respect to the retinal vessels (Enalapril Maleate:  $p < 0.001$  for T1,  $p < 0.001$  for T2; Pyrogallin:  $p$  value not significant for T1,  $p < 0.001$  for T2; Albendazole:  $p$  not significant for both T1 and T2,

most likely due to small sample size, Mebendazole: p not significant for T1,  $p < 0.05$  for T2; Zearalenone:  $p < 0001$  for T1,  $p < 0.001$  for T2. Trunk vessel thickness is provided for the T1 treatment only. The trunk vessel thickness measurements also yielded statistically significant values for albendazole  $p < 0.01$  and mebendazole  $p < 0.001$ . (C) Confocal images of transverse sections through control and chemically-treated retinae, showing the organization of neuronal layers. Retinal ganglion cells including the optic nerve and photoreceptors are visualized with Zn-8 and Zpr-1 antibodies, respectively (both in red) and intraocular vessels are marked by GFP expression (green). To visualize plexiform layers, sections were counterstained with fluorophore-conjugated phalloidin (blue). The concentrations of chemicals used for experiments shown in these panels are indicated in Table 1 in italics.

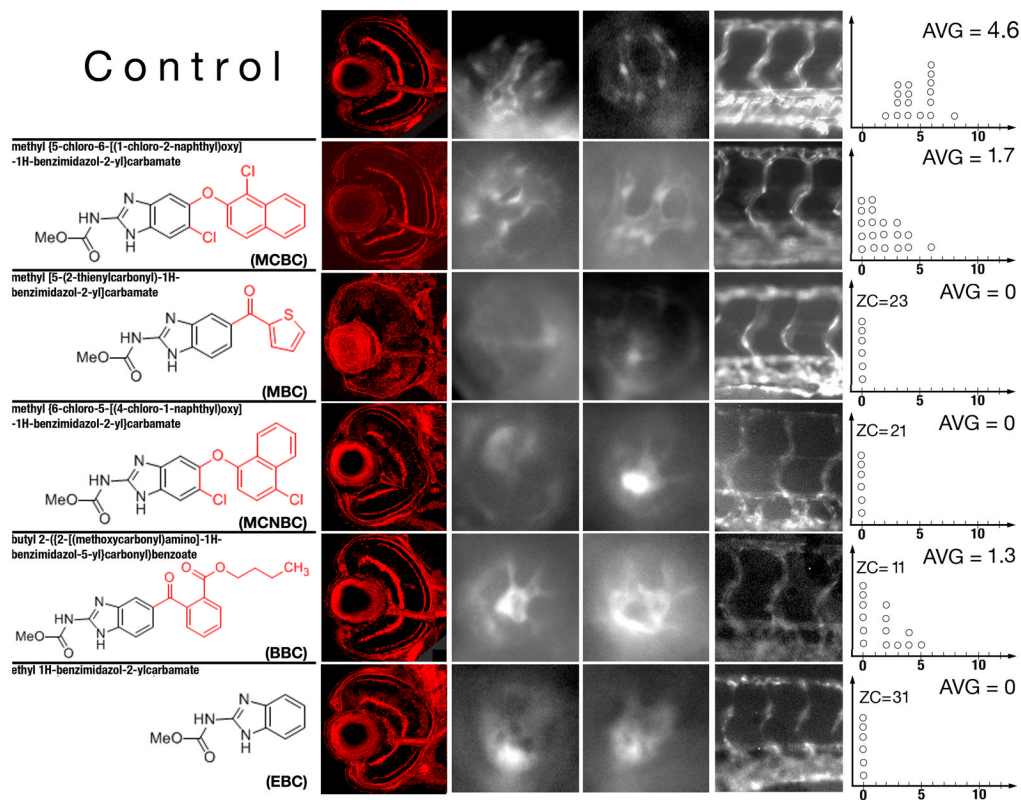


**Fig. 5.** Phenotypic changes produced by compounds structurally similar to albendazole and mebendazole. The left-most column of panels shows confocal images of transverse sections through control and chemically-treated retinæ. The concentrations of chemicals used for experiments shown in these panels are indicated in Table 2 in italics. Panels in the middle two columns of images show lateral views of the retinal vasculature through the lens at 96 hpf. The right-most column of images shows lateral views of the trunk vasculature. Graphs to the right are plotted as in Fig. 4. In all images, dorsal is up and anterior is left.

Summary of phenotypic changes produced by different dilutions of chemicals in the retina and trunk. Appropriate dilutions (provided in parentheses) were prepared and used to treat embryos (C1–C7). X represents the “T1” concentration from Fig 4. It is the highest concentration tested that produces phenotype in the retina but not in the trunk. Its molar value is indicated next to each compound name. In each table cell, font is color-coded as follows: blue indicates concentrations that do not affect retinal lamination; red indicates concentrations that cause defects of the retinal architecture; black indicates concentrations for which we did not test retinal lamination. At high concentrations, all chemicals are toxic, and cause death followed by a rapid decomposition of larvae (cells in grey). At somewhat lower concentrations, fish lack heart beat but the GFP signal persists in blood vessels (cells in orange). These animals are also considered dead. As concentrations are lowered further, the compounds do not affect the heart beat but trunk and/or retina vessels are affected (cells in yellow). The concentrations that do not produce any obvious phenotypic changes in this assay are indicated in light green.

Table 1

	C1	C2	C3	C4	C5	C6	C7
Eye	Enalapril Maleate (x = 100 $\mu$ M)						
	Normal (0.031X)	Normal (0.062X)	Normal (0.12X)	Normal (0.25X)	Thick vessels (0.5X)	Thick vessels (X)	Fish decomposed (2X)
Trunk	Normal (0.031X)	Normal (0.062X)	Normal (0.12X)	Normal (0.25X)	Normal (0.5X)	Normal (X)	Fish decomposed (2X)
Eye	Pyrogallin (x = 60 $\mu$ M)						
	Normal (0.125X)	Fewer Vessels (0.25X)	Fewer Vessels (0.5X)	Fewer Vessels (X)	Fewer Vessels (2X)	Fish decomposed (4X)	Fish decomposed (8X)
Trunk	Normal (0.125X)	Normal (0.25X)	Normal (0.5X)	Normal (X)	Partial vessel loss (2X)	Fish decomposed (4X)	Fish decomposed (8X)
Eye	Albendazole (x = 9 $\mu$ M)						
	Fewer Vessels (0.25X)	Fewer Vessels (0.5X)	Fewer Vessels (X)	Fewer Vessels (5X)	Fewer Vessels (10X)	Fish decomposed (20X)	Fish decomposed (40X)
Trunk	Normal (0.25X)	Normal (0.5X)	Normal (X)	Partial vessel loss (5X)	Partial vessel loss (10X)	Fish decomposed (20X)	Fish decomposed (40X)
Eye	Mebendazole (x = 4 $\mu$ M)						
	Fewer Vessels (0.5X)	Fewer Vessels (X)	Fewer Vessels (10X)	Fewer Vessels (10X)	Fewer Vessels, fish dead (20X)	Fish decomposed (40X)	Fish decomposed (80X)
Trunk	Normal (0.5X)	Normal (X)	Partial vessel loss (2X)	Partial vessel loss (10X)	Partial vessel loss, fish dead (20X)	Fish decomposed (40X)	Fish decomposed (80X)
Eye	Zearalenone (x = 8 $\mu$ M)						
	Normal (0.25X)	Thick vessels (0.5X)	Thick vessels (X)	Thick vessels, fish dead (5X)	Fish decomposed (10X)	Fish decomposed (20X)	Fish decomposed (40X)
Trunk	Normal (0.25X)	Normal (0.5X)	Normal (X)	Normal vessels, fish dead (5X)	Fish decomposed (10X)	Fish decomposed (20X)	Fish decomposed (40X)

Table 2

Compounds structurally similar to albendazole and mebendazole. Content, formatting, and color codes are as in Table 1.

	C1	C2	C3	C4	C5	C6	C7
Eye	methyl 5-chloro-6-[(1-chloro-2-naphthyl)oxy]-1H-benzimidazol-2-yl]carbamate (MCBC) (x = Normal (0.12X))	Normal (0.25X)	Fewer Vessels (0.5X)	Fewer Vessels (X)	Fewer Vessels, fish dead (2X)	Fish decomposed (4X)	Fish decomposed (8X)
Trunk	Normal (0.12X)	Normal (0.25X)	Normal (0.5X)	Normal (X)	Partial vessel loss, fish dead (2X)	Fish decomposed (4X)	Fish decomposed (8X)
Eye	methyl 5-(2-thienylcarbonyl)-1H-benzimidazol-2-yl]carbamate (MBC) (x = 2.1 μM)	Absent, fish dead (2X)	Absent, fish dead (4X)	Absent, fish dead (20X)	Fish decomposed (40X)	Fish decomposed (80X)	Fish decomposed (160X)
Trunk	Partial vessel loss (X)	Fewer Vessels, fish dead (2X)	Fewer Vessels, fish dead (4X)	Fewer Vessels, fish dead (20X)	Fish decomposed (40X)	Fish decomposed (80X)	Fish decomposed (160X)
Eye	methyl 6-chloro-5-[(4-chloro-1-naphthyl)oxy]-1H-benzimidazol-2-yl]carbamate (MCNBC) (x = 30 μM)	Normal (0.12X)	Normal (0.25X)	Absent (X)	Absent (2X)	Fish decomposed (4X)	Fish decomposed (8X)
Trunk	Normal (0.12X)	Normal (0.25X)	Normal (0.5X)	Normal (X)	Partial vessel loss, fish dead (2X)	Fish decomposed (4X)	Fish decomposed (8X)
Eye	butyl 2-[(12-(methoxycarbonyl)amino)-1H-benzimidazol-5-yl]carbonyl]benzoate (BBC) (x = Normal (0.062X))	Normal (0.125X)	Normal (0.25X)	Fewer Vessels (0.5X)	Fewer Vessels (X)	Fewer Vessels, fish dead (2X)	Fish decomposed (4X)
Trunk	Normal (0.062X)	Normal (0.125X)	Normal (0.25X)	Normal (0.5X)	Normal (X)	Fewer Vessels, fish dead (2X)	Fish decomposed (4X)
Eye	ethyl 1H-benzimidazol-2-yl]carbamate (EBC) (x = 70 μM)	Normal (0.125X)	Normal (0.25X)	Absent (X)	Absent, fish dead (2X)	Fish decomposed (4X)	Fish decomposed (8X)
Trunk	Normal (0.125X)	Normal (0.25X)	Normal (0.5X)	Normal (X)	Absent, fish dead (2X)	Fish decomposed (4X)	Fish decomposed (8X)